Mechanism for period-doubling bifurcation in a semiconductor laser subject to optical injection

Thomas Erneux
Université Libre de Bruxelles, Optique Nonlinéaire Théorique, Campus Plaine, C.P. 231, 1050 Bruxelles, Belgium

Vassilios Kovanis,* Athanasios Gavrielides,† and Paul M. Alsing‡
Nonlinear Optics Center, Phillips Laboratory, PL/LIDN, 3350 Aberdeen Avenue SE, Kirtland Air Force Base, New Mexico 87117-5776
(Received 25 January 1995)

The single-mode rate equations for a semiconductor laser subject to optical injection are investigated analytically. We determine the first branch of periodic solutions for low values of the injection field. For larger values of the injection field, we derive a third-order pendulum equation for the phase difference of the laser field of the form $\psi'''+\psi'=\Lambda\cos(\psi)$, where Λ groups all the key laser parameters. This equation captures several aspects of the numerical bifurcation diagram, namely, the fixed amplitude of the period-one solution and the period-doubling bifurcation. Finally, we compute the optical power spectrum utilizing the perturbation solutions of the phase equation before and after the period-doubling transition. We also obtain very good agreement with the numerically computed spectrum.

PACS number(s): 42.55.Px, 05.45.+b

I. INTRODUCTION

Experimentally observed spectra of a laser diode subject to strong injection have been reproduced numerically using a single-mode injection model by Simpson *et al.* [1,2]. The numerical study allows a detailed analysis of a period-doubling route to chaos and has clarified the role of the linewidth enhancement factor. Of particular interest is the fact that period doubling appears at relatively low values of the injection field. The main objective of this paper is to capture analytically the mechanism leading to these period-doubling instabilities and to obtain simple analytical expressions of the optical power spectra. To this end, we propose an asymptotic approximation of the laser equations based on two large parameters, namely, the ratio of the carrier to the photon lifetimes and the linewidth enhancement factor. We obtain a simple nonlinear problem that exhibits the dominant role of the phase of the laser field. This particular feature of the semiconductor laser with an injected signal has been discussed before by Lang [3] and has been suspected by Winful and Wang [4] and Winful [5] for coupled semiconductor lasers. However, the actual mechanism of how the phase induces the first two bifurcations has never been analyzed.

The single-mode rate equations used successfully in [1,2] to compute the optical power spectra consist of three equations for the amplitude of the electrical field E, the phase difference between master and slave electrical fields ψ, and the carrier density above threshold N. They are given by

$$\frac{dE}{d\tau}=NE+\eta\cos(\psi), \tag{1.1}$$

$$\frac{d\psi}{d\tau}=\Delta-bN-\eta E^{-1}\sin(\psi), \tag{1.2}$$

$$T\frac{dN}{d\tau}=P-N-P(1+2N)E^2. \tag{1.3}$$

In these equations, time τ is measured in units of the photon lifetime ($\tau=t/t_p$, where $t_p\approx10^{-12}$ s). T is defined as the ratio of the carrier to the photon lifetimes ($T=t_s/t_p$, where $t_s\approx10^{-9}$ s). b is the linewidth enhancement factor ($b\approx3-4$). η is proportional to the amplitude of the injected field and is the control parameter. P is the pumping current above threshold [$P=0.375$ is proportional to $(J/J_{\rm th}-1)$, where J and $J_{\rm th}$ denote the pumping current and the pumping current at threshold, respectively]. Δ is the frequency offset of the master laser from the free-running frequency of the slave laser. In this system of equations the nonlinear gain was not included in order to simplify the analytical calculations.

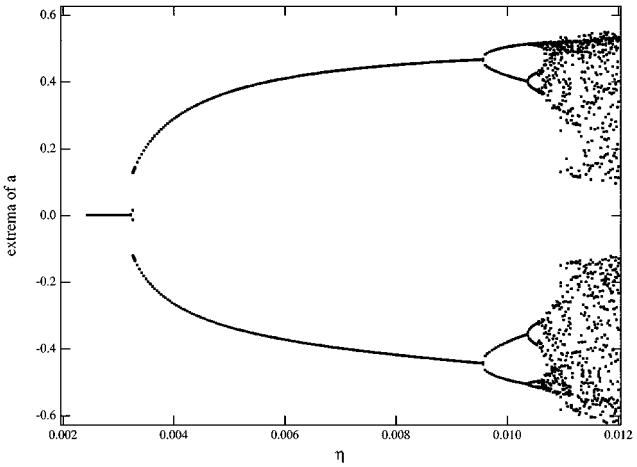

FIG. 1. Bifurcation diagram of the periodic solutions for the experimentally determined parameters. The values of the parameters are $T=155$, $b=4$, and $P=0.375$.

*Also at the Department of Mathematics and Statistics, University of New Mexico, Albuquerque, NM 87131. Electronic address: kovanis@xaos.plk.af.mil
†Electronic address: tom@photon.plk.af.mil
‡Electronic address: alsing@arom.plk.af.mil

A typical bifurcation diagram of the possible solutions of Eqs. (1.1)−(1.3) is shown in Fig. 1 for zero detuning ($\Delta=0$). The figure represents $\alpha=(E/E_s)-1$ as a function of η for the experimental parameter values extracted with the four-wave-mixing technique [6] and used in the numerical simulations [1,2]. From low to moderate values of η, we note a cascade of period-doubling bifurcations. We also note from the time evolution that the oscillations remain nearly harmonic. This contrasts the pulsating oscillations observed in other cases of period doubling in class B laser systems [7,8]. In this paper, we concentrate on the first two bifurcations, namely, a Hopf bifurcation at a relatively low value of η, and the first period-doubling bifurcation, which occurs as the amplitude of the Hopf bifurcation branch saturates to a constant. We consider the case $\Delta=0$ in detail and then discuss the effect of $\Delta\neq 0$. The fact that T, the ratio of the two fundamental time scales, is a large quantity $O(\sim 10^2$–$10^3)$ suggests an approximation of the laser equations (1.1)–(1.3). This approximation must be derived carefully because the limit of large T is singular.

The paper is organized as follows. In Sec. II we eliminate the large-T singularity by reformulating the laser equations in terms of deviations from the nonzero intensity solution. In Sec. III we determine a branch of periodic solutions that emerges from a Hopf bifurcation as the injection field is progressively increased. The fact that this Hopf bifurcation appears at a very low value of the control parameter is explained by considering the large-b limit. Furthermore, this limit allows us to explain why the amplitude of the periodic solutions saturates at a fixed value as the control parameter is further increased. The results described in Sec. III then motivate an asymptotic analysis of the laser equations, assuming a specific scaling between T and b. This is done in Sec. IV where we derive a third-order pendulum equation for the phase of the laser field and obtain an approximation of the first period-doubling bifurcation. We compute the optical spectra in Sec. V. Section VI discusses the effect of detuning (Δ) and summarizes the main results. All mathematical details are deferred to the Appendixes for clarity.

II. FORMULATION

In the case of a free-running laser ($\eta=0$), we note from the linearized theory that small perturbations from the steady-state solution $E_s=1$ and $N_s=0$ are oscillating with relaxation frequency $\omega_R\approx(2P/T)^{1/2}$ and are slowly decaying with damping rate $\gamma_R\approx(1+2P)/2T$. We also note from the solution of the linearized problem that N is $\sim O(T^{-1/2})$, while $E-1$ remains $O(1)$ as $T\to\infty$. This suggests the reformulation of the laser equations in terms of new variables defined as

$$s=(2P/T)^{1/2}\tau, \tag{2.1}$$

$$E=1+\alpha, \tag{2.2}$$

and

$$N=(2P/T)^{1/2}n, \tag{2.3}$$

where the factor $(2P)^{1/2}$ has been introduced in (2.3) so that the leading-order equations as $T\to\infty$ do not depend on any parameter. We consider small values of the injected signal and scale η as

$$\eta=T^{-1}\lambda. \tag{2.4}$$

This scaling is motivated by the linearized theory, which indicates that the first Hopf bifurcation appears at $\eta_{H1}=O(T^{-1})$ [9]. Note that there is a second Hopf bifurcation located at $\eta_{H2}=O(T^{-1/2})$. The basic steady-state solution is unstable for $\eta_{H1}<\eta<\eta_{H2}$ and cascading period-doubling bifurcations are observed as soon as $\eta>\eta_{H1}$. In this paper, we only consider the case $\eta=O(T^{-1})$. After introducing (2.1)–(2.4) into Eqs. (1.1)–(1.3), we obtain the following equations for α, ψ, and n:

$$\alpha'=n(1+\alpha)+\epsilon\lambda\,\cos(\psi), \tag{2.5}$$

$$\psi'=-bn-\frac{\epsilon\lambda}{\alpha+1}\sin(\psi), \tag{2.6}$$

$$n'=-(\alpha+\tfrac{1}{2}\alpha^2)-\epsilon n[1+2P(1+\alpha)^2], \tag{2.7}$$

where the prime means differentiation with respect to s and ϵ is defined by

$$\epsilon=(2PT)^{-1/2}\ll 1. \tag{2.8}$$

Because $\epsilon=O(T^{-1/2})$ is small, we investigate Eqs. (2.5)–(2.7) in the limit $\epsilon\to 0$. If $\epsilon=0$, Eqs. (2.5)–(2.7) reduce to the following problem for $\alpha=\alpha_0$, $n=n_0$, and $\psi=\psi_0$:

$$\alpha_0'=n_0(\alpha_0+1), \tag{2.9}$$

$$n_0'=-(\alpha_0+\tfrac{1}{2}\alpha_0^2), \tag{2.10}$$

$$\psi_0'=-bN_0. \tag{2.11}$$

These equations can be integrated once. We find the integrals

$$E_0=\tfrac{1}{2}(1+\alpha_0)^2-\ln(1+\alpha_0)+n_0^2 \tag{2.12}$$

and

$$C_0=\psi_0+b\,\ln(1+\alpha_0), \tag{2.13}$$

where E_0 and C_0 are the constants of integration [10]. An analysis of the solutions of Eqs. (2.9) and (2.10) in the phase plane shows that these equations admit a one-parameter family of periodic solutions for all $E_0>0$. We denote by (α_0,n_0) the P-periodic solution of Eqs. (2.9) and (2.10). Equation (2.13) implies that ψ_0 is P periodic because α_0 is P periodic, but its mean value is arbitrary since C_0 is arbitrary. In order to find how E_0 and C_0 depend on the bifurcation parameter λ, we formulate solvability conditions for the higher-order terms multiplying ϵ in Eqs. (2.5)–(2.7). These conditions are formulated in Appendix A and are given by

$$\int_0^P\left[\frac{2\alpha_0+\alpha_0^2}{1+\alpha_0}\lambda\,\cos(\psi_0)-2n_0^2[1+2P(1+\alpha_0)^2]\right]ds=0 \tag{2.14}$$

and

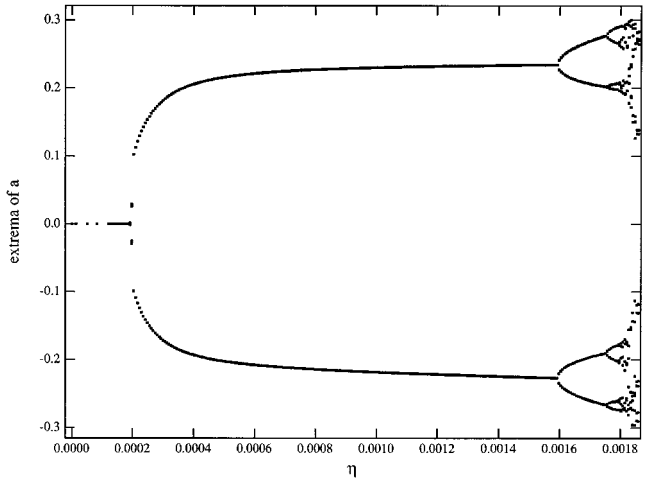

FIG. 2. Bifurcation diagram of the periodic solutions for T large and b large. The values of the parameters are $T=1000$, $b=10$, and $P=0.375$.

$$\int_0^P [-\sin(\psi_0)+b\ \cos(\psi_0)]\ \frac{1}{1+\alpha_0}\ ds=0. \quad (2.15)$$

In the next section, we investigate these conditions in detail and determine the first branch of periodic solutions.

III. HOPF BIFURCATION

Equations (2.14) and (2.15) are called the bifurcation equations because they relate the amplitude of the periodic solutions (proportional to E_0) and the bifurcation parameter λ. They cannot be solved analytically because we do not have an explicit expression for α_0 and n_0. However, the numerical bifurcation diagram shown in Fig. 1 indicates that the amplitude of the Hopf bifurcation branch remains small and quickly approaches a constant amplitude as η increases. By considering successive larger values of b, we have noted numerically that the amplitude of α is clearly a quantity $\sim b^{-1}$ and the saturation of the amplitude after a thin layer near the Hopf bifurcation point becomes more transparent. See Fig. 2. This suggests the determination of a small-amplitude solution of Eqs. (2.9) and (2.10), assuming $\alpha_0=O(b^{-1})$, $n_0=O(b^{-1})$, and $\psi_0=O(1)$ as $b\to\infty$. All details are given in Appendix B. The leading expressions for α_0, n_0, and ψ_0 are given by

$$\alpha_0=a\ \sin(s), \quad n_0=a\ \cos(s),$$

and

$$\psi_0=ba\ \sin(s) \quad (3.1)$$

where $a=O(b^{-1})$. Substituting (3.1) into the conditions (2.14) and (2.15) and assuming that

$$\lambda=O(b^{-1}) \quad (3.2)$$

leads to the following conditions for amplitude a and C_0:

$$\lambda\ \sin(C_0)2aJ_1(ab)-a^2(1+2P)=0, \quad (3.3)$$

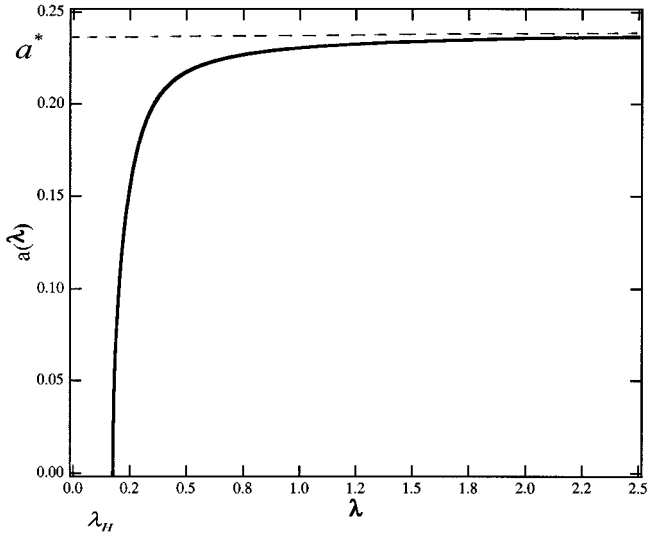

FIG. 3. Period-one solution. The period-one branch of the solution is given by $\alpha\approx a\ \sin(s)$, $n\approx a\ \cos(s)$, and $\psi\approx C+ba\ \sin(s)$. The figure represents the amplitude $a(\lambda)$ and is defined by (3.5). The branch is first quasivertical near the Hopf bifurcation point $\lambda=\lambda_H$ and then saturates at a constant amplitude $a=a^*=2.4b^{-1}$.

$$\cos(C_0)bJ_0(ab)-\sin(C_0)[baJ_1(ba)+J_0(ab)]=0, \quad (3.4)$$

where the Bessel functions come from the expansion of $\cos(\psi_0)=\cos[ba\ \sin(s)]$ in Fourier series [11]. Eliminating C_0 from these equations gives an implicit amplitude equation for $a=a(\lambda)$:

$$\lambda=\frac{a(1+2P)}{2J_1(ab)}\left[1+\frac{1}{b^2J_0^2(ab)}\,[baJ_1(ba)+J_0(ab)]^2\right]^{1/2}. \quad (3.5)$$

This function is shown in Fig. 3. As $a\to 0$, we note from (3.5) that λ approaches a constant given by

$$\lambda_H=b^{-1}(1+2P)+O(b^{-3}). \quad (3.6)$$

We have verified that (3.6) matches the exact expression of the Hopf bifurcation point obtained from the linearized theory and evaluated for b large [8]. We also note from (3.5) that $\lambda\to\infty$ as $a\to a^*$, where $x=a^*b$ is defined as the first zero of the Bessel function $J_0(x)$. In a first approximation a^* is given by

$$a^*\approx 2.4b^{-1}. \quad (3.7)$$

In summary, we have shown that the amplitude of the Hopf bifurcation branch quickly approaches a constant value as $\lambda=O(1)$. In the next section, we consider $\lambda=O(1)$, assume a specific scaling between b and T, and determine an approximation for the first period-doubling bifurcation.

IV. PERIOD-DOUBLING BIFURCATION

In Sec. III we found that a branch of periodic solutions emerges from a Hopf bifurcation at $\lambda_H=O(b^{-1})$ and quickly approaches a constant $O(b^{-1})$ amplitude as $\lambda=O(1)$. In this section we investigate the bifurcation dia-

gram for $\lambda=O(1)$ in detail. To this end, we assume the scalings

$$\lambda=O(1), \quad \alpha=O(b^{-1}), \quad n=O(b^{-1}),$$

and

$$\psi=O(1). \tag{4.1}$$

In addition, we introduce a specific scaling between ϵ (equivalently $T^{-1/2}$) and b^{-1}:

$$\epsilon=O(b^{-1}). \tag{4.2}$$

This scaling is motivated by the numerical values of ϵ and b, which were used for the bifurcation diagram in Fig. 2 (i.e., $\epsilon=4\times10^{-2}$ and $b^{-1}=10^{-1}$). Using (4.1) and (4.2), we find from Eqs. (2.5)–(2.7) that the leading order solution satisfies the equations

$$\alpha'=n+\epsilon\lambda\ \cos(\psi), \tag{4.3}$$

$$\psi'=-bn, \tag{4.4}$$

$$n'=-\alpha. \tag{4.5}$$

Equivalently, we may eliminate α and obtain two equations for n and ψ:

$$n''+n=-\epsilon\lambda\ \cos(\psi), \tag{4.6}$$

$$\psi'=-bn. \tag{4.7}$$

Equations (4.6) and (4.7) reveal the main effect of injection. If $\lambda=0$ (no injection), the laser is described in first approximation as a harmonic oscillator. If $\lambda\neq0$, the phase of the laser field produces the essential nonlinearity leading to instabilities. It is mathematically interesting to formulate an equation for ψ only. From (4.6) and (4.7), we eliminate n and obtain the equivalent third-order equation for ψ

$$\psi'''+\psi'=\Lambda\ \cos(\psi), \tag{4.8}$$

where $\Lambda=O(1)$ is defined by

$$\Lambda=\epsilon b\lambda=b\,\eta T^{1/2}(2P)^{-1/2}. \tag{4.9}$$

This is the main mathematical result of this paper. Equation (4.8) has appeared in a different area of physics as a geometrical model for dentrite growth but with very specific boundary conditions [12].

The original laser exhibits cascading period-doubling bifurcations and we are interested in determining periodic solutions of Eq. (4.8). We have found numerically that Eq. (4.8) admits a branch of periodic solutions characterized by an almost constant amplitude and a first period-doubling bifurcation located at

$$\Lambda=\Lambda_{\rm PD}\approx0.62. \tag{4.10}$$

Figure 4 represents $\eta_{\rm PD}=(2P)^{1/2}T^{-1/2}b^{-1}\Lambda_{\rm PD}$ as a function of b. The points in the figure are the numerical values of $\eta_{\rm PD}$ computed from the original equations (1.1)–(1.3). As expected, we note that our approximation becomes better for large b. We next investigate Eq. (4.8) in detail and determine

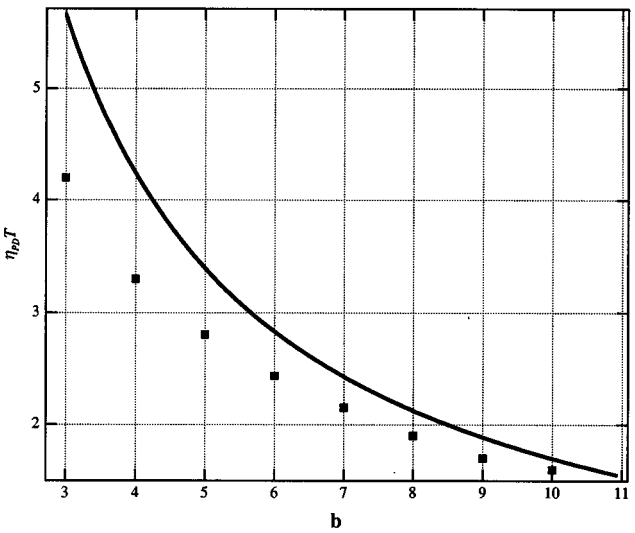

FIG. 4. Period-doubling bifurcation point. The figure compares the exact values of the period-doubling bifurcation points (solid squares) with the asymptotic approximation $\eta_{\rm PD}T=(2PT)^{1/2}b^{-1}0.62$ (full line).

analytical expressions for $\eta_{\rm PD}$ as well as the period-one and period-two branches of solutions.

A. Period-one solution

An approximation of the period-one solution is obtained by a perturbation analysis. See Appendix C. In the first approximation, we find that

$$\psi_{P1}=C+D\ \sin(S)+O(\Lambda), \tag{4.11}$$

where $S=[1+O(\Lambda)]s$. C is equal to 0 or π and $D\approx2.4$ is the first root of the Bessel function $J_0(x)$. Figure 5 represents the exact and approximate solutions for $C=0$ and $\Lambda=0.6171$. This value of Λ is slightly below the period-doubling bifurcation point located at $\Lambda\approx0.62$. Note that the general solution of Eq. (4.8) is quasiperiodic. In order to obtain a bounded periodic solution, we have integrated the modified equation

$$\psi'''+\psi'=\Lambda\ \cos(\psi)-\zeta\psi'' \tag{4.12}$$

for successive smaller values of ζ (from $\zeta=0.1$ to 0.05). The additional term in (4.12) is suggested by the higher-order damping term in the original equations [specifically, the term $-\epsilon n(1+2P)$ in Eq. (2.7), which leads to a term proportional to ψ'' in the phase equation (4.12)].

B. Period-doubling bifurcation point

In order to determine a possible bifurcation point from the period-one solution, we consider the linearized problem for the period-one solution:

$$u'''+u'=-\Lambda\ \sin(\psi_{P1})u, \tag{4.13}$$

where $u=\psi-\psi_{P1}$ is defined as the small perturbation. A period-doubling bifurcation located at $\Lambda=\Lambda_{\rm PD}$ corresponds to a period-two solution of Eq. (4.13). In Appendix D we determine an approximation for $\Lambda_{\rm PD}$ that matches the nu-

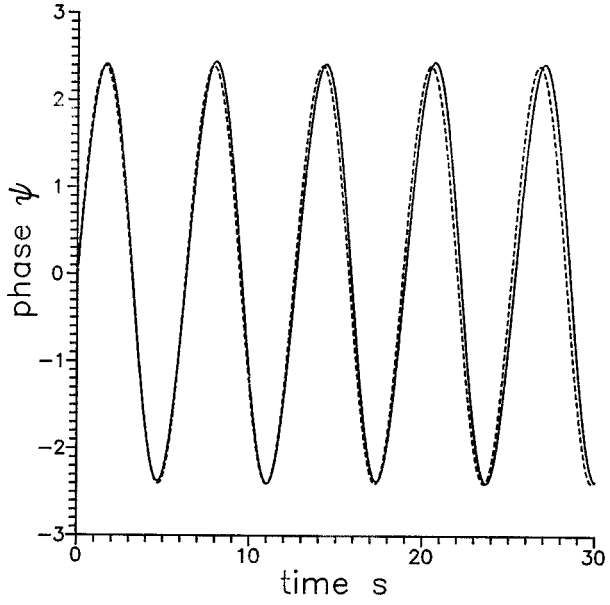

FIG. 5. Approximation of the period-one solution of the phase equation. The full line represents the period-one solution of Eq. (4.8) for a value of Λ before the period-doubling bifurcation point $\Lambda_{PD}\approx 0.62$ ($\Lambda=0.6171$). The dotted line is the approximation (4.11), i.e., $\psi=2.4\sin(s)$. The progressive shift between the two curves as time increases is due to the fact that our approximation neglects the small nonlinear change of the frequency.

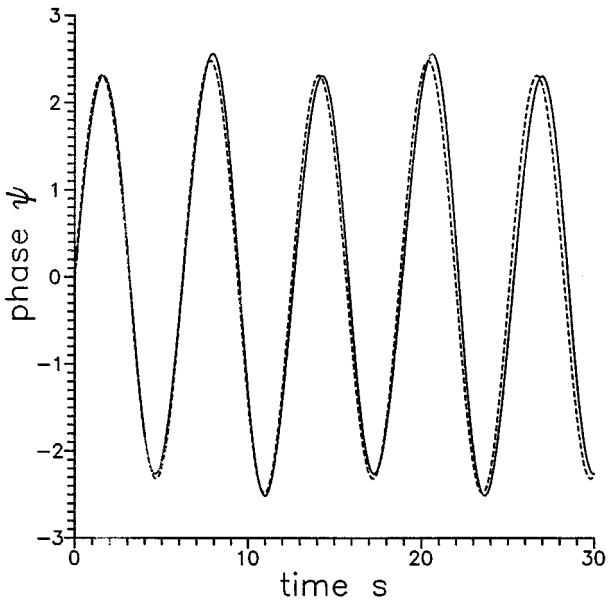

FIG. 6. Period-two solution. The period-two solution of Eq. (4.8) is represented for a value of Λ slightly above the period-doubling bifurcation point ($\Lambda=0.6208$). Note the periodic alternation of the maxima and minima, which allows us to recognize the period-two solution. The dotted line denotes the approximation $\psi=2.4\sin(s-s_0)-0.1\{\cos[(s-s_0)/2]-0.17\cos[3(s-s_0)/2]\}$, where s_0 is introduced so that $\psi(0)=0$.

merical estimate (4.10) for the case $C=0$. The period-two solution of Eq. (4.13) is obtained from a four-term Fourier expansion. We find an approximate solution given by

$$u\approx\cos(S/2)+r\cos(3S/2), \tag{4.14}$$

where $r\approx-0.17$.

C. Period-two solution

We now investigate the period doubling bifurcation. In Appendix E we seek a solution of the nonlinear problem of the form

$$\psi=\psi_{P1}+v, \tag{4.15}$$

where ψ_{P1} is given by (4.11) and v is small. The linearized theory suggests the search for a solution of the form $v=Au$, where u is defined by (4.14) and A is an unknown amplitude. We obtain

$$v\approx[12(\Lambda-\Lambda_{PD})/\Lambda_{PD}]^{1/2}[\cos(S/2)+r\cos(3S/2)], \tag{4.16}$$

where $\Lambda_{PD}\approx 0.62$. The bifurcation is clearly supercritical since (4.16) only exists if $\Lambda>\Lambda_{PD}$. Figure 6 represents the period-two solution for a value Λ slightly above the period-doubling bifurcation point and is compared to the approximation (4.15) and (4.16). The high accuracy that is required for the determination of Λ_{PD} prevents us from making a complete quantitative comparison. The amplitude of v in (4.16) has been fixed arbitrarily to -0.1. This implies $\Lambda-\Lambda_{PD}=5\times10^{-4}$, which then implies $\Lambda_{PD}=0.6203$.

V. OPTICAL POWER SPECTRA

Direct experimental evidence of the successive bifurcations is difficult because the intensity oscillates in the gigahertz regime. In practice, the bifurcation diagram is reconstructed from Fourier spectra obtained using a scanning Fabry-Pérot spectrum analyzer [1,2]. In this section, we obtain analytical expressions for the optical power spectra. The optical power spectrum is defined by

$$F(\omega)=|S(\omega)|^2, \tag{5.1}$$

where

$$S(\omega)=\int_{-\infty}^{\infty}\exp(-i\omega s)(1+\alpha)\exp(i\psi)ds, \tag{5.2}$$

where $E=(1+\alpha)\exp(i\psi)$ is the complex electrical field expressed as a function of time s, where s is the original time scaled by the relaxation frequency of the free-running laser, i.e., $s=\omega_R\tau=(2P/T)^{1/2}\tau$. α and ψ satisfy Eqs. (2.5)–(2.7). Figures 7(a) and 7(b) show the exact numerical spectra for the period-one and period-two solutions, respectively. The period-two solution is computed near the period-doubling bifurcation point. By comparing the two figures, we clearly note in Fig. 7(b) the emergence of the subharmonic frequencies located at $\omega\approx\pm n/2$ ($n=1,2,...$).

We now determine analytical expressions for these spectra using the asymptotic approximation of the solution valid for T and b large. For the period-one solution, recall that $\alpha=O(b^{-1})\ll 1$ and $\psi\approx D\sin(s)$, where D is defined as the first zero of the Bessel function $J_0(x)$. Using the generating function of the Bessel functions [11], i.e.,

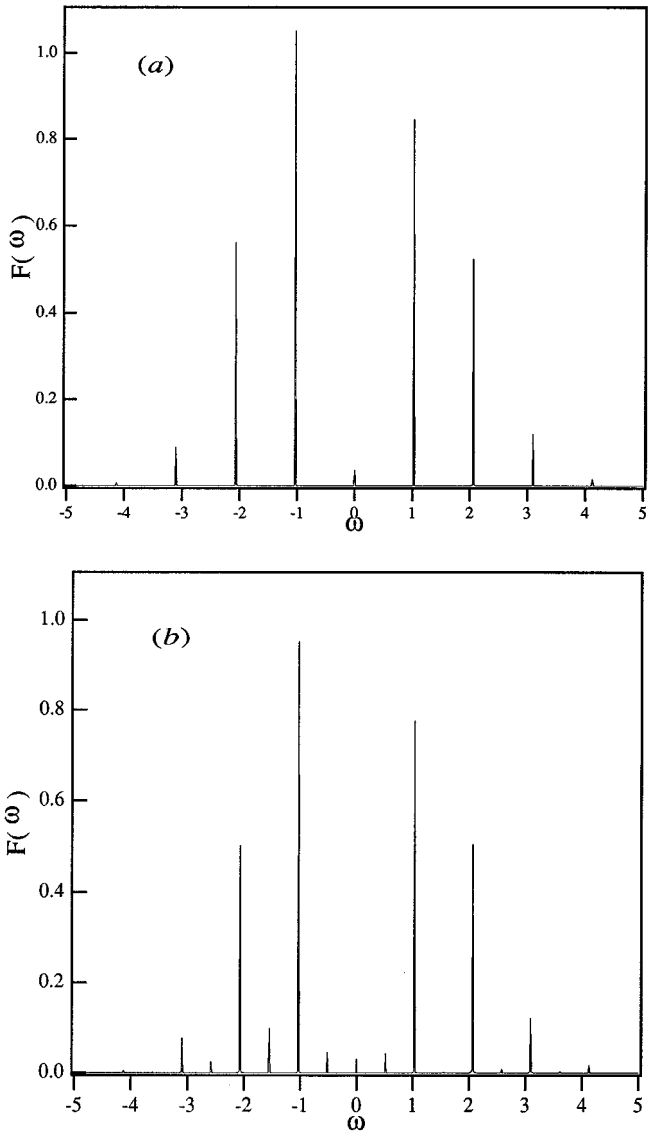

FIG. 7. Optical power spectra. Represented are the numerical power spectra for (a) $\eta=1.4\times10^{-3}$ and (b) $\eta=1.62\times10^{-3}$. The other parameters are $T=1000$, $b=10$, and $P=0.375$.

$$\exp[iD\ \sin(s)]=\sum_{m=-\infty}^{\infty} J_m(D)\exp(ims), \tag{5.3}$$

we obtain from (5.2) that

$$S(\omega)\approx\sum_{m=-\infty}^{\infty} J_m(D)\,\delta(\omega-m), \tag{5.4}$$

where $\delta(x)$ denotes the delta function. Substituting (5.4) into (5.1) gives a power spectrum that exhibits peaks centered at $\omega=\pm m$ of size $J_m^2(D)$. Note that there is no contribution at $m=0$ since $J_0(D)=0$. This explains the small contribution at the center line in Fig. 7(a). If $m\neq0$, the analysis predicts symmetric side bands. The apparent asymmetry in Fig. 7(a) can be explained by taking into account the $O(\Lambda)$ correction term for ψ (see Appendic C). Specifically, we have computed $S(\omega)$ using $\psi=D\ \sin(s)+B\ \sin(2s)$, where $B=-\Lambda J_2(D)/3$, and found good agreement with the numerically computed spectrum.

A similar analysis is possible for the period-two solution. The simplest approximation is given by (4.16) for the period-two solution near the period-doubling bifurcation point. We have the approximation $\alpha=O(b^{-1})\ll1$ and $\psi\approx D\ \sin(s)+R\ \cos(s/2)$. From (5.2) and using (5.3) twice, we obtain

$$S(\omega)\approx\sum_{m=-\infty}^{\infty} J_m(D)\sum_{n=-\infty}^{\infty} J_n(R)e^{in\pi/2}\delta(\omega-m-n/2). \tag{5.5}$$

Substituting (5.5) into (5.1), we find that there is no contribution at $\omega=0$, the $\omega=\pm1$ peaks have size $J_1^2(D)J_0^2(R)$ $[\approx J_1^2(D)]$, and the new peaks at $\omega=\pm\frac{1}{2}$ have size $J_1^2(D)J_1^2(R)$ $[\approx J_1^2(D)R^2]$.

VI. SUMMARY AND DISCUSSION

Our asymptotic analysis is based on two large parameters that appear in the dimensionless laser equations. The parameter T is the ratio of the carrier to the photon lifetimes and is equivalent to the ratio of the cavity to the inversion of population lifetimes for gas or solid-state lasers. For many practical lasers this ratio is a large quantity. Thus our analysis of the large-T limit (Sec. II) should apply to other lasers as well. The parameter b is the linewidth enhancement factor and is typically a semiconductor laser parameter. Our analysis of the large-b limit could be useful for a gas laser with an injected signal [14–16], but only for a particular range of values for the cavity and atomic detunings.

From a mathematical point of view, the key point of our analysis was the derivation of a third-order pendulum equation for the phase of the laser field [i.e., Eq. (4.8)]. In particular, this equation revealed the destabilizing mechanism for small injection but sufficiently large values of the linewidth enhancement factor b. A different aspect of the bifurcation problem is revealed by the equivalent equations for the carrier density and the phase of the laser field, respectively [i.e., Eqs. (4.6) and (4.7)]. The laser behaves as a harmonic oscillor, but is driven by a phase that depends on the state of the oscillator. Thus it is the phase that introduces the essential feedback nonlinearity leading to instabilities.

The case of nonzero detunings ($\Delta\neq0$) can be analyzed by a similar method. We find that the response of the laser is described by the phase equation

$$\psi'''+\psi'=\overline{\Delta}+\Lambda\ \cos(\psi), \tag{6.1}$$

where Λ is defined by (4.9) and $\overline{\Delta}=\Delta T^{1/2}(2P)^{-1/2}$ is proportional to Δ. This equation is similar to Eq. (4.8) and we expect similar results if $|\Delta|$ is small and $\Lambda=O(1)$. We are currently investigating the case where $|\Delta|$ and Λ are both $O(1)$.

ACKNOWLEDGMENTS

This research was supported by the U.S. Air Force Office of Scientific Research Grant No. AFOSR-93-1-0084, the National Science Foundation Grant No. DMS-9308009, the Fonds National de la Recherche Scientifique (Belgium), and the Inter University Attraction Pole of the Belgian government. P.M.A. wishes to thank the National Research Council for supporting this work.

APPENDIX A: BIFURCATION EQUATIONS

In this appendix we derive the bifurcation equations for the periodic solutions (α_0,n_0,ψ_0) of Eqs. (2.5)–(2.7). To this end, we introduce the functions $E=E(\alpha,n)$ and $C=C(\psi,\alpha)$ defined by

$$E=\tfrac{1}{2}(1+\alpha)^2-\ln(1+\alpha)+n^2, \tag{A1}$$

$$C=\psi+b\ \ln(1+\alpha). \tag{A2}$$

These functions are motivated by the first integrals (2.12) and (2.13). If $\epsilon=0$, we know that $E=E_0$ and $C=C_0$ are constants. If $\epsilon\neq 0$ and small, we expect that E' and C' are proportional to ϵ. We obtain differential equations for E and C by differentiating (A1) and (A2) and using Eqs. (2.5)–(2.7). We find

$$E'=\epsilon\left[\frac{2\alpha+\alpha^2}{1+\alpha}\,\lambda\ \cos(\psi)-2n^2[1+xJ(1+\alpha)^2]\right] \tag{A3}$$

and

$$C'=\epsilon\lambda[-\sin(\psi)+b\ \cos(\psi)]\ \frac{1}{1+\alpha}. \tag{A4}$$

We now require that E and C are bounded periodic functions of s as $\epsilon\to 0$. This implies the conditions (2.14) and (2.15) (standard averaging).

APPENDIX B: SMALL-AMPLITUDE SOLUTIONS

In this appendix we apply the Poincaré-Lindstedt method [13] and determine a small-amplitude solution of Eqs. (2.9) and (2.10) of the form

$$\alpha_0(S,a)=a\alpha_1(S)+a^2\alpha_2(S)+\cdots, \tag{B1}$$

$$n_0(S,a)=an_1(S)+a^2n_2(S)+\cdots, \tag{B2}$$

where

$$S=(1+a^2\sigma+\cdots)s \tag{B3}$$

and a is a small parameter defined as the amplitude of the critical mode

$$a=\frac{1}{\pi}\int_0^{2\pi}\alpha_0(S,a)\sin(S)\,dS. \tag{B4}$$

Introducing (B1)–(B3) into Eqs. (2.9) and (2.10) and equating to zero, the coefficients of each power of a lead to a sequence of problems for the unknown coefficients. Solving these equations, we obtain

$$\begin{aligned}\alpha_0&=a\ \sin(S)-a^2[\tfrac{1}{4}+\tfrac{5}{12}\ \cos(2S)]+O(a^3),\\ n_0&=a\ \cos(S)+a^2\tfrac{1}{3}\ \sin(2S)+O(a^3).\end{aligned} \tag{B5}$$

The frequency correction σ is obtained from a solvability condition and is given by

$$\sigma=-\tfrac{1}{6}. \tag{B6}$$

The expression for ψ_0 is then obtained by substituting (B5) into (2.11):

$$\psi_0=C_0-b\ \ln(1+\alpha_0)=C_0-ba\ \sin(S)+O(ba^2). \tag{B7}$$

With (B7), we may determine $\cos(\psi_0)$ and $\sin(\psi_0)$, which appear in the bifurcation equations. We find [11]

$$\begin{aligned}\cos(\psi_0)&=\cos[C_0-ba\ \sin(S)]+O(ba^2)\\ &=\cos(C_0)[J_0(ab)+2J_2(ab)\cos(2S)+\cdots]\\ &\quad+\sin(C_0)[2J_1(ab)\sin(S)\\ &\quad+2J_3(ab)\sin(3S)+\cdots]\end{aligned} \tag{B8}$$

and

$$\begin{aligned}\sin(\psi_0)&=\sin[C_0-ba\ \sin(S)]+O(ba^2)\\ &=\sin(C_0)[J_0(ab)+2J_2(ab)\cos(2S)+\cdots]\\ &\quad-\cos(C_0)[2J_1(ab)\sin(S)\\ &\quad+2J_3(ab)\sin(3S)+\cdots],\end{aligned} \tag{B9}$$

where $J_n(x)$ denotes a Bessel function of order n.

APPENDIX C: PERIOD-ONE SOLUTION OF EQ. (4.8)

We seek a 2π periodic solution of Eq. (4.8) of the form

$$\psi(S,\Lambda)=\psi_0(S)+\Lambda\psi_1(S)+\cdots, \tag{C1}$$

where

$$S=(1+\Lambda^2\sigma+\cdots)s. \tag{C2}$$

Introducing (C1) and (C2) into Eq. (4.8) leads to a succession of problems for the unknown coefficients given by

$$O(1)\ \psi_0'''+\psi_0'=0, \tag{C3}$$

$$O(\Lambda)\ \psi_1'''+\psi_1'=\cos(\psi_0), \tag{C4}$$

$$O(\Lambda^2)\ \psi_2'''+\psi_2'=-\sin(\psi_0)\,\psi_1-3\sigma\psi_0'''-\sigma\psi_0', \tag{C5}$$

where the prime means differentiation with respect to S. The solution of Eq. (C3) is

$$\psi_0=C+D\ \sin(S), \tag{C6}$$

where we have defined the time origin so that ψ_0 has no contribution proportional to $\cos(S)$. $\cos(\psi_0)$ is needed for the $O(\Lambda)$ problem and is given by

$$\begin{aligned}\cos(\psi_0)&=\cos(C)[J_0(D)+2J_2(D)\cos(2S)+\cdots]\\ &\quad-\sin(C)[2J_1(D)\sin(S)+\cdots],\end{aligned} \tag{C7}$$

where the missing terms correspond to higher-order harmonics. Because C and D are unknown, we next consider Eq. (C4). This equation must satisfy two solvability conditions

because the homogeneous problem admits two solutions [namely, $\psi_1=C_1$ and $\psi_1=D_1\exp(\pm iS)$]. Using (C7), these conditions require that

$$J_0(D)=0$$

and

$$\sin(C)=0. \tag{C8}$$

Equivalently, (C8) implies that $D\approx 2.4$ is the first zero of the Bessel function $J_0(x)$ and

$$C=0 \quad \text{or} \quad \pi. \tag{C9}$$

We next determine the solution of Eq. (C4) and obtain

$$\psi_1=C_1+(D_1e^{iS}+\text{c.c.})-\tfrac{1}{3}\cos(C)J_2(D)\sin(2S)+\cdots . \tag{C10}$$

We have found C and D, but the frequency correction σ is still unknown. Therefore, we examine Eq. (C5). To this end, we need $\sin(\psi_0)$, given by

$$\sin(\psi_0)=2\cos(C)J_1(D)\sin(S)+\cdots . \tag{C11}$$

Then the solvability conditions for Eq. (C5) give

$$\overline{D_1}=D_1, \quad C_1=0,$$

and

$$\sigma=-\frac{1}{6D}J_1(D)J_2(D)+\cdots . \tag{C12}$$

Thus we have found that D_1 is real, C_1 is zero, and we have obtained the correction of the frequency σ.

APPENDIX D: PERIOD-DOUBLING BIFURCATION POINT

In this appendix we seek a solution of Eq. (4.13) with ψ_{P1} given by (4.11) using a four-term Fourier series

$$u=\alpha e^{iS/2}+\beta e^{-iS/2}+\gamma e^{3iS/2}+\delta e^{-3iS/2}. \tag{D1}$$

Substituting (D1) into Eq. (4.13) with $\sin(\psi_{P1})=\sin[C+D\sin(S)]\approx 2\cos(C)J_1(D)\sin(S)$, where $C=0$ or π, leads to four equations for the coefficients of $\exp(\pm iS/2)$ and $\exp(\pm 3iS/2)$:

$$\tfrac{3}{8}\alpha=\Lambda\cos(C)J_1(D)(\beta-\gamma), \tag{D2}$$

$$\tfrac{3}{8}\beta=\Lambda\cos(C)J_1(D)(\alpha-\delta), \tag{D3}$$

$$\tfrac{15}{8}\gamma=-\Lambda\cos(C)J_1(D)\alpha, \tag{D4}$$

$$\tfrac{15}{8}\delta=-\Lambda\cos(C)J_1(D)\beta. \tag{D5}$$

Eliminating γ and δ leads to two equations for α and β. The condition for nontrivial solution then requires that

$$\tfrac{8}{15}[\cos(C)\Lambda J_1(D)]^2+\cos(C)\Lambda J_1(D)-\tfrac{3}{8}=0, \tag{D6}$$

which admits the roots $\cos(C)\Lambda J_1(D)=x_+\approx 0.32$ and $x_-\approx -2.20$. Thus we have two cases. Either

$$C=0, \quad \Lambda=\Lambda_{\text{PD}}=0.32/J_1(D)\approx 0.62 \tag{D7}$$

or

$$C=\pi, \quad \Lambda=\Lambda_{\text{PD}}=2.2/J_1(D)\approx 4.23, \tag{D8}$$

where we use $J_1(D)=J_1(2.4)\approx 0.52$. Note that the solution at $\Lambda=\Lambda_{\text{PD}}$ verifies

$$\alpha=\beta, \quad \gamma=\delta, \quad \gamma=r\alpha, \tag{D9}$$

where

$$r=-\tfrac{8}{15}x_+\approx -0.17. \tag{D10}$$

Thus the solution (D1) can be rewritten as

$$u=2\alpha[\cos(S/2)+r\cos(3S/2)]. \tag{D11}$$

APPENDIX E: PERIOD-TWO SOLUTION

We now concentrate on the case $C=0$ and determine an approximation of the period-two solution. We seek a solution of the form

$$\psi=\psi_{P1}+v, \tag{E1}$$

where ψ_{P1} is given by (4.11) with $C=0$ and v is assumed small. Substituting (E1) into Eq. (4.8) gives

$$v'''+v'=-\Lambda\sin(\psi_{P1})v-\tfrac{1}{2}\Lambda\cos(\psi_{P1})v^2+\tfrac{1}{6}\Lambda\sin(\psi_{P1})v^3+\cdots . \tag{E2}$$

Using

$$\sin(\psi_{P1})\approx 2J_1(D)\sin(s), \tag{E3}$$

$$\cos(\psi_{P1})\approx 2J_2(D)\cos(2s), \tag{E4}$$

we determine an approximation for v of the form of (D11) given by

$$v=A[\cos(S/2)+r\sin(S/2)], \tag{E5}$$

where $A\ll 1$ and r are unknown. Inserting (E5) into Eq. (E2) and equating to zero, the coefficients of $\exp(iS/2)$ and $\exp(iS/3)$ lead to the conditions

$$-\tfrac{3}{8}A=-\Lambda J_1A(1-r)+\frac{\Lambda}{3}J_1\frac{A^3}{8}(2-3r+6r^2-3r^3), \tag{E6}$$

$$\tfrac{15}{8}Ar=-\Lambda J_1A+\Lambda J\frac{A^3}{18}(1+r+2r^2), \tag{E7}$$

where $J_1=J_1(D)$. From (E7), we obtain r as

$$r=-\tfrac{8}{15}\Lambda J_1+O(A^2\Lambda J_1). \tag{E8}$$

Then, from (E6), we find

$$A[-\tfrac{3}{8}+\Lambda J_1(1+\tfrac{8}{15}\Lambda J_1)]=A^3[\tfrac{1}{12}\Lambda J_1+O((\Lambda J_1)^2)]. \tag{E9}$$

The coefficient of A on the left-hand side of Eq. (E9) is identical to the expression (D6) with $C=0$ for the period-doubling bifurcation point. In the vicinity of $\Lambda=\Lambda_{\rm PD}=0.62$, we evaluate (E9) and obtain A as

$$A\approx[12(\Lambda-\Lambda_{\rm PD})/\Lambda_{\rm PD}]^{1/2}, \tag{E10}$$

which implies that the period-two solution is only defined for $\Lambda>\Lambda_{\rm PD}$.

[1] T. B. Simpson, J. M. Liu, A. Gavrielides, V. Kovanis, and P. M. Alsing, Appl. Phys. Lett. **64**, 3539 (1994).

[2] T. B. Simpson, J. M. Liu, A. Gavrielides, V. Kovanis, and P. M. Alsing, Phys. Rev. A **51**, 4181 (1995); V. Kovanis, A. Gavrielides, T. B. Simpson, and J. M. Liu, Appl. Phys. Lett. **67**, 2780 (1995).

[3] R. Lang, IEEE J. Quantum Electron. **QE-18**, 976 (1982).

[4] H. G. Winful and S. S. Wang, Appl. Phys. Lett. **53**, 1894 (1988).

[5] H. G. Winful, Phys. Rev. A **46**, 6093 (1992).

[6] T. B. Simpson and J. M. Liu, J. Appl. Phys. **73**, 2587 (1993); J. M. Liu and T. B. Simpson, IEEE Photonics Technol. Lett. **4**, 380 (1993); IEEE J. Quantum Electron. **30**, 957 (1994).

[7] I. B. Schwartz and T. Erneux, SIAM J. Appl. Math. **54**, 1083 (1994).

[8] D. Pieroux, T. Erneux, and K. Otsuka, Phys. Rev. A **50**, 1822 (1994).

[9] From the linearized theory, we determine two Hopf bifurcation given by $\eta_{H1}=(1+2P)(1+b^2)^{1/2}T^{-1}(b^2-1)^{-1}$ and $\eta_{H2}=[(b^2-1)P]^{1/2}T^{-1/2}$.

[10] T. Erneux (unpublished).

[11] *Handbook of Mathematical Functions*, edited by M. Abramowitz and I. Stegun, 9th ed. (Dover, New York, 1972).

[12] M. D. Kruskal and H. Segur, Stud. Appl. Math. **85**, 129 (1991).

[13] J. Kervokian and J. D. Cole, in *Perturbation Methods in Applied Mathematics*, Applied Mathematical Sciences Vol. 34 (Springer-Verlag, Berlin, 1981).

[14] D. K. Bandy, L. M. Narducci, and L. A. Lugiato, J. Opt. Soc. Am. B **2**, 148 (1985); Y. Gu, D. K. Bandy, J.-M. Yuan, and L. N. Narducci, Phys. Rev. A **31**, 354 (1985).

[15] G. L. Oppo, A. Politi, G. L. Lippi, and F. T. Arecchi, Phys. Rev. A **34**, 4000 (1986); A. Politi, G. L. Oppo, and R. Badii, *ibid*. **33**, 4055 (1986); H. Solari and G. L. Oppo, Opt. Commun. **111**, 173 (1994).

[16] P. A. Braza and T. Erneux, Phys. Rev. A **41**, 6470 (1990).